

# The mystery of superconductivity in the cuprates evinced by London penetration depths measurements

T. Schneider

*Physik-Institut der Universität Zürich, Winterthurerstrasse 190,  
CH-8057 Zürich, Switzerland*

The London penetration depth plays a key role in determining and uncovering many properties of a superconductor, including homogeneity, anisotropy, isotope effects, importance of quantum and thermal fluctuations, and facets of the nature of superconductivity in a particular material. Guided by the generic phase diagram in the temperature-dopant concentration plane we examine experimental data on the temperature, isotope substitution, inhomogeneity and magnetic field dependence of the penetration depths to uncover some facets of the mystery of superconductivity in the cuprates.

To appear in Proceedings of the International School of Physics, Enrico Fermi Course CLV, The Physics of Complex Systems.

The London penetration depth is a fundamental quantity of a superconductor. It plays a key role in determining and uncovering many properties of a superconductor, including homogeneity, anisotropy, isotope effects, importance of quantum and thermal fluctuations, and facets of the nature of superconductivity in a particular material. In recent years experimental data on the temperature, dopant concentration, magnetic field and oxygen isotope mass dependence of the penetration depth became available for a variety of cuprate superconductors. Here we analyze and discuss the experimental data, guided by the generic phase diagram of the cuprates, depicted in Fig.1. After passing the so called underdoped limit ( $p_u \approx 0.05$ ), where  $p$  is the hole concentration,  $T_c$  reaches its maximum value  $T_c^m$  at  $p_m \approx 0.16$ . With further increase of  $p$ ,  $T_c$  decreases and finally vanishes in the overdoped limit  $p_o \approx 0.27$  [1,2]. There is the line  $T_c(p)$  of finite temperature phase transitions, separating the superconducting and non-superconducting states, with critical endpoints at  $p_u$  and  $p_o$ . Here  $T_c$  vanishes and the cuprates undergo at zero temperature doping ( $p$ ) tuned quantum phase transitions. As their nature is concerned, resistivity measurements reveal a quantum superconductor to insulator (QSI) transition in the underdoped limit ( $p_u$ ) and in the overdoped limit ( $p_o$ ) a quantum superconductor to normal state (QSN) transition. Another essential experimental fact is the doping dependence of the anisotropy. In tetragonal cuprates it is defined as the ratio  $\gamma = \lambda_c/\lambda_{ab}$  of the London penetration depths due to supercurrents flowing perpendicular ( $\lambda_c$ ) and parallel ( $\lambda_{ab}$ ) to the  $ab$ -planes. Approaching the QSN transition  $\gamma$  remains finite, while at the QSI transition it tends to infinity [3,4]. When  $\gamma$  remains finite the system exhibits anisotropic but genuine three dimensional (3D)-, while  $\gamma \rightarrow \infty$  implies 2D-behavior. The resulting competition between anisotropy and superconductivity raises serious doubts whether 2D mechanisms and models, corresponding to the limit  $\gamma = \infty$ , can explain the essential observations of superconductivity in the cuprates [4]. There is mounting evidence that close to the phase transition line  $T_c(p)$  thermal fluctuations dominate, while quantum fluctuations dominate both, the QSI and QSN transitions. Furthermore, due to the 3D to 2D crossover, tuned by the rise of  $\gamma$  with reduced dopant concentration, these fluctuations are enhanced. For these reasons, mean-field treatments, including the BCS theory are expected to apply far from the critical line only. This singles out the low temperature region around optimum doping  $p_m$ .

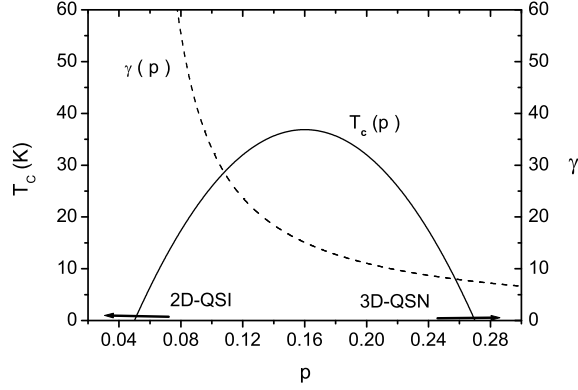


FIG. 1. Schematic phase diagram of cuprate superconductors. Variation of  $T_c$  and  $\gamma(T=0) = \lambda_c(T=0)/\lambda_{ab}(T=0)$  with hole concentration  $p$ . Quantum phase transitions occur at the endpoints  $p = p_u \simeq 0.05$  and  $p = p_o \simeq 0.27$  of the critical line  $T_c(p)$ . At  $p_u$  a two dimensional quantum superconductor to insulator (2D-QSI)- and at  $p_o \simeq 0.27$  3D quantum superconductor to normal state (3D-QSN)- transition occurs.

In the mean-field approximation the London penetration depth of an anisotropic superconductor in the Meissner state is given by [5,6]

$$\frac{1}{\lambda_i^2(T)} \cong \frac{e^2}{\pi^2 \hbar c^2} \oint dS_F \frac{\mathbf{v}_{F_i} \mathbf{v}_{F_i}}{|\mathbf{v}_F|} \left( 1 + 2 \int_{\Delta_k}^{\infty} dE_k \frac{\partial f(E_k)}{\partial E_k} \frac{E_k}{\sqrt{E_k^2 - \Delta_k^2}} \right). \quad (1)$$

$dS_{F, \mathbf{v}_{F_i}}$  and  $|\mathbf{v}_F|$  are respectively the surface element of the Fermi surface, Fermi velocity in direction  $i$  and the magnitude of the Fermi velocity.  $f(E_k)$  is the Fermi function and  $\Delta_k$  the energy gap in direction  $k$ . The  $i$  index refers to the principal crystallographic directions  $a$ ,  $b$  and  $c$ . The second term which is negative, describes the decrease of  $1/\lambda_i^2(T)$  caused by the thermal population of Bogoliubov quasi-particle levels with energy  $E_k$ , and it is this quantity where the anisotropy and magnitude of the energy gap enters. In this approximation  $1/\lambda_i^2(T)$  vanishes close to  $T_c$  as  $1/\lambda_i^2(T) = 1/\lambda_{i0}^2 (1 - T/T_c)^\nu$  with  $\nu = 1/2$ , while there is mounting evidence for  $\nu \simeq 2/3$  in the experimentally accessible regime. Thus close to  $T_c$  where thermal fluctuations dominate the mean field treatment fails. Otherwise, e.g. at sufficiently low temperatures and far away from the QSI and QSN transitions the neglect of fluctuations appears to be justified. Here Eq.(1) reduces for noninteracting quasiparticle excitations around the four d-wave nodes, which dominate the leading low temperature behavior, to [7]

$$\frac{1}{\lambda_{ab}^2(T)} = \frac{1}{\lambda_{ab}^2(0)} (1 - AT), \quad A = \lambda_{ab}^2(0) \ln 2 \frac{k_B e^2 v_F}{\hbar^2 c^2 d v_2}, \quad \frac{1}{\lambda_i^2(0)} \cong \frac{e^2}{\pi^2 \hbar c^2} \oint dS_F \frac{\mathbf{v}_{F_i} \mathbf{v}_{F_i}}{|\mathbf{v}_F|}. \quad (2)$$

The Fermi velocities  $v_F$  and  $v_2$  enter the quasiparticles excitation energies  $E_k = \hbar \sqrt{v_F^2 k_1^2 + v_2^2 k_2^2}$  and refer to velocities along directions normal and tangential to the Fermi surface at each node.  $d$  is the mean interlayer spacing along the  $c$ -axis. The velocity ratio  $v_F/v_2$  is a fundamental material parameter which measures the anisotropy of the quasiparticle excitation spectrum. This scenario is not restricted to the penetration depth. It predicts simple power-law temperature dependencies in the thermodynamic and transport properties at sufficiently low temperatures. For example, the penetration depth measurements find that  $1/\lambda_{ab}^2$  exhibits in the clean limit and at low temperature a linear temperature dependence [8,9], in agreement with Eq.(2). The NMR relaxation rate exhibits the expected  $T^3$  temperature dependence [10]. The predicted effect of impurities in giving rise to a universal thermal conductivity [11,12] has been confirmed [13]. The clean-limit specific heat varying as  $T^2$  appears to have been observed [14–16].

For a spherical Fermi surface, one recovers for the zero temperature penetration depth the standard result,  $1/\lambda^2(T=0) = 4\pi n e^2 / (m c^2)$ , where  $n$  is the number density of the electrons in the normal state [17]. In recent years the penetration depth has been the subject of intense experimental investigation in high- $T_c$  compounds [18–24]. It has become the practice to associate the anisotropy with anisotropic effective masses  $m_i^*$  and to interpret the experimental data in terms of the London formula

$$\frac{1}{\lambda_i^2(0)} = \frac{4\pi n_s e^2}{m_i^* c^2} \quad (3)$$

by introducing the number density  $n_s$  of the superfluid. In a real superconductor, the ionic potential modifies the spherical Fermi surface of free electrons drastically. In this case it is not evident what should be taken for the effective mass  $m_i^*$  and the number density  $n_s$ . Although, using Eqs.(2) and (3), we can define the ratio  $n_s/m_i^*$ , which often has been used to interpret experimental results, in terms of

$$\frac{1}{\lambda_i^2(0)} \cong \frac{e^2}{\pi^2 \hbar c^2} \oint dS_F \frac{\mathbf{v}_F \cdot \mathbf{v}_F}{|\mathbf{v}_F|} = \frac{4\pi n_s e^2}{m_i^* c^2} \frac{n_s}{m_i^*}. \quad (4)$$

This relation shows that  $n_s/m_i$  is just a way of parameterizing experimental results, with no discernible connection to the band mass or carrier concentration. Indeed in the mean-field approximation  $1/\lambda_i^2(0)$  is determined by normal state properties, namely the integral of the Fermi velocity over the Fermi surface. Noting that in high- $T_c$  superconductors band structure calculations [25] and ARPES [26,27] studies uncovered drastic deviations from the free electron picture it is evident that interpretations based on the ratio  $n_s/m_i^*$  obscure the origin of the anisotropy  $\gamma_{ij} = \lambda_i/\lambda_j$  and the doping dependence of the zero temperature penetration depth, as well as the isotope effect on this quantity. Indeed, an inspection of Eq.(2) leads to the conclusion that the anisotropy stems from flat portions of the Fermi surface, while the doping dependence reflects that of the Fermi surface. On the other hand, there is little doubt about the importance of residual electron-electron and electron-phonon interactions, not accounted for in Eq.(2). Quantifying these interactions is difficult in the normal state of the cuprates, given the lack of well-defined single-particle excitations as revealed by various experiments. Contrariwise, well-defined quasiparticle excitations do exist in the superconducting state, and a description of the low temperature state in terms of superfluid Fermi liquid theory is believed to apply. Fermi-liquid corrections account for the Fermi-liquid interactions between electrons. In the superconductor their effect is the renormalization of the Fermi velocity ratio in terms of  $\mathbf{v}_F/v_2 \rightarrow \alpha^2 \mathbf{v}_F/v_2$  [7], where  $\mathbf{v}_F/v_2$  is the bare value entering Eq.(2). The comparison of  $d\lambda^{-2}/dT$  at  $T = 0$  in Bi2212, evaluated with Eq.(2) and the ARPES estimate for  $\mathbf{v}_F/v_2$  [26] with the value deduced from penetration depth measurements [28] points to a substantial Fermi liquid renormalization, namely  $\alpha^2 \approx 0.3$ , due to interactions between the nodal quasiparticles in the superconducting state. To explore the doping dependence of the renormalization we invoke the empirical relation  $T_c d/dT (\lambda_{ab}^2(0)/\lambda_{ab}^2(T))|_{T=0} \approx -0.6$  [9], which applies to variety of cuprates with  $T_c$  ranging from 30 to 130K and dopant concentrations extending from the underdoped to the optimally doped regime. It implies with the empirical relation,  $T_c \propto 1/\lambda_{ab}^2(0)$  [23], established for underdoped cuprates, and Eq.(2) that  $\alpha^2 \mathbf{v}_F/v_2$  is nearly doping independent.

Much less attention has been devoted to the renormalization of the Fermi velocity due to electron-phonon interaction. Isotope substitution, i.e. the exchange of  $^{18}\text{O}$  by  $^{16}\text{O}$  is a suitable probe, whereby the lattice parameters remain essentially unaffected [29,30], while the phonon frequencies associated with the mass of the oxygen ions, or more generally, the oxygen lattice degrees of freedom are modified [31]. In recent years the isotope effect on the zero temperature penetration depth has been investigated, using a variety of techniques. In Table I we listed the experimental estimates for the relative change

$$\frac{\Delta \lambda_{ab}^2(\tilde{T})}{\lambda_{ab}^2(\tilde{T})} = \frac{n \lambda_{ab}^2(\tilde{T}) - m \lambda_{ab}^2(\tilde{T})}{m \lambda_{ab}^2(\tilde{T})}, \quad (5)$$

upon isotope exchange for various cuprates and  $\text{MgB}_2$ , where  $n = ^{18}\text{O}$ ,  $m = ^{16}\text{O}$  in the cuprates and  $n = ^{11}\text{B}$ ,  $m = ^{10}\text{B}$  in  $\text{MgB}_2$ . The data also reveals that within experimental accuracy  $\Delta \lambda_{ab}^2(\tilde{T})/\lambda_{ab}^2(\tilde{T}) = \Delta \lambda_{ab}^2(0)/\lambda_{ab}^2(0)$ . At zero temperature and taking the anisotropy of the quoted materials into account ( $\lambda_c \gg \lambda_a \approx \lambda_b$ ) the mean-field expression (2) reduces to

$$\frac{1}{\lambda_{ab}^2(T=0)} \cong \frac{e^2}{\pi^2 \hbar c^2 \sqrt{2}} \oint dS \mathbf{v}_{F_{ab}}. \quad (6)$$

Since the lattice parameters remain essentially unaffected [29,30] by isotope exchange, while the dynamics, associated with the mass of the respective ions, are modified, the substantial isotope effect on the zero temperature penetration depth requires a renormalization of the normal state Fermi velocity  $\mathbf{v}_F \rightarrow \tilde{\mathbf{v}}_F = \mathbf{v}_F/(1+f)$  where  $\mathbf{v}_F$  is the bare velocity and  $f$  the electron-phonon coupling constant which changes upon oxygen isotope exchange in the cuprates but remains nearly unaffected by boron isotope substitution in  $\text{MgB}_2$ . However, in the Migdal-Eliashberg [33] (ME) treatment of the electron-phonon interaction the coupling constant  $f$  is independent of the ionic masses and assumed to be small [34,35]. This is true if the parameter  $\omega_0 f/E_F$  is small, where  $\omega_0$  is the relevant phonon frequency and  $E_F$  the Fermi energy. Thus the isotope effect on the penetration depth is expected to be small, of the order of the

adiabatic parameter  $\tilde{\gamma} = \omega_0/E_F \ll 1$ . The ME theory retains terms only of order 0. Cuprates, however, have Fermi energies much smaller than those of conventional metals [36] so that  $\tilde{\gamma}$  is no longer negligible small. Thus the large oxygen isotope effects on the zero temperature in-plane penetration depth in the cuprates, listed in Table I, poses a fundamental challenge to this understanding and calls for a theory that goes beyond ME [37,38].

	$T_c(\text{K})$	$\tilde{T}$	$\Delta\lambda_{ab}^2(\tilde{T})/\lambda_{ab}^2(\tilde{T})$	Ref
YBa <sub>2</sub> Cu <sub>3</sub> O <sub>7-<math>\delta</math></sub>	89.0	10	0.05	[20]
Y <sub>0.7</sub> Pr <sub>0.3</sub> Ba <sub>2</sub> Cu <sub>3</sub> O <sub>7-<math>\delta</math></sub>	60.6	5	0.13	
Y <sub>0.6</sub> Pr <sub>0.4</sub> Ba <sub>2</sub> Cu <sub>3</sub> O <sub>7-<math>\delta</math></sub>	45.3	5	0.11	
YBa <sub>2</sub> Cu <sub>3</sub> O <sub>7-<math>\delta</math></sub> (film)	89.3	4	0.05	[21]
La <sub>2-x</sub> Sr <sub>x</sub> CuO <sub>4+<math>\delta</math></sub> , $x = 0.08$	19.5	0	0.10(2)	[19]
La <sub>2-x</sub> Sr <sub>x</sub> CuO <sub>4+<math>\delta</math></sub> , $x = 0.086$	22.4	0	0.08(1)	
Bi <sub>1.6</sub> Pb <sub>0.4</sub> Sr <sub>2</sub> Ca <sub>2</sub> Cu <sub>3</sub> O <sub>10+<math>\delta</math></sub>	107	0	0.05	[18]
MgB <sub>2</sub>	38.5	0	0.02(2)	[24]

Table I: Experimental estimates for  $\Delta\lambda_{ab}^2(\tilde{T})/\lambda_{ab}^2(\tilde{T}) = \left( {}^n\lambda_{ab}^2(\tilde{T}) - {}^m\lambda_{ab}^2(\tilde{T}) \right) / {}^m\lambda_{ab}^2(\tilde{T})$  with  $n = {}^{18}\text{O}$ ,  $m = {}^{16}\text{O}$  in the cuprates and  $n = {}^{11}\text{B}$ ,  $m = {}^{10}\text{B}$  in MgB<sub>2</sub>

Indeed, the relative shifts  $\Delta\lambda_{ab}^2(\tilde{T})/\lambda_{ab}^2(\tilde{T})$  are substantial and surprisingly close to  $({}^{18}M_o - {}^{16}M_o)/{}^{16}M_o = 0.125$ . This differs fundamentally from the behavior of optic O - phonon frequencies. The expected behavior,  $\omega \propto M^{-1/2}$ , was confirmed in YBa<sub>2</sub>Cu<sub>3</sub>O<sub>7- $\delta$</sub>  by measuring the frequency shift of the transverse optic phonons (copper-oxygen stretching modes), yielding  $\Delta\omega/\omega \approx -0.06$ , in agreement with  $\Delta\omega/\omega \approx ({}^{16}M_o/{}^{18}M_o)^{1/2} - 1 = -0.057$  [31]. In any case the observed oxygen isotope effect on the zero temperature penetration depth uncovers together with Eq.(6), a substantial renormalization of the normal state Fermi velocity due to oxygen lattice degrees of freedom, while in MgB<sub>2</sub> this renormalization due to boron isotope exchange turns out to be marginal. This renormalization is also expected to affect the superconducting properties. Taking the empirical relation  $T_c d/dT (\lambda_{ab}^2(0)/\lambda_{ab}^2(T))|_{T=0} \approx -0.6$  [9] for granted, Eq.(2) implies that

$$\frac{\Delta T_c}{T_c} = -\frac{\Delta A}{A} = -\frac{\Delta\lambda_{ab}^2(0)}{\lambda_{ab}^2(0)} - \frac{\Delta(\widetilde{v_F/v_2})}{(\widetilde{v_F/v_2})}, \quad (7)$$

where  $\widetilde{v_F/v_2}$  is the bare ratio, renormalized with respect to electron-phonon coupling. Noting that close to optimum doping  $\Delta T_c/T_c$  is negligible small, the oxygen isotope exchange uncovers a substantial electron-phonon renormalization of  $\widetilde{v_F/v_2}$ , characterizing the quasiparticles in the superconducting state. Indeed, close to optimum doping  $\Delta(\widetilde{v_F/v_2})/(\widetilde{v_F/v_2}) \cong -\Delta\lambda_{ab}^2(0)/\lambda_{ab}^2(0)$  holds and this quantity varies from 0.05 to 0.11 (see Table I). This effect, providing direct evidence of the relevance of electron-phonon coupling in the superconducting state, should be observable with ARPES. Noting that thermally excited quasiparticles destroy superconductivity by driving  $1/\lambda_{ab}^2(T)$  to zero, we can estimate  $T_c$  by extrapolating Eq.(2) to  $1/\lambda_{ab}^2(T) = 0$ . This yields  $T_c A \approx 1$  and confirms Eq.(7). In this context it is interesting to note that details of the Fermi-surface topology of deuterated  $\kappa$ -(BEDTTTF)<sub>2</sub>Cu(NCS)<sub>2</sub> have been measured as a function of pressure and compared with equivalent measurements of the undeuterated salt. The data suggest that the negative isotope effect observed on deuteration is due to small differences in Fermi-surface topology caused by the isotopic substitution [32].

Close to the phase transition line  $T_c(p)$  thermal critical fluctuations, neglected in mean-field treatments, dominate the thermodynamic properties. Approaching the phase transition line around  $p = p_m$  from below (see Fig.1), there is mounting evidence that the critical behavior of homogeneous cuprates falls in the experimentally accessible temperature regime into the 3D-XY universality class [4,39–52]. Here critical 3D-XY fluctuations dominate because the fluctuations of the vector potential are strongly suppressed due to the small value of the effective charge of the pairs [39]. In the 3D-XY universality class the transition temperature  $T_c$ , the critical amplitude of the specific heat  $A^-$  and the critical amplitudes of the penetration depths  $\lambda_{i0}$  are universally related by [50]

$$(k_B T_c)^3 = \left( \frac{\Phi_0^2 R^-}{16\pi^3} \right)^3 \frac{1}{\lambda_{a0}^2 \lambda_{b0}^2 \lambda_{c0}^2 A^-}. \quad (8)$$

$R^- \simeq 0.815$  is a universal number. The critical amplitudes are defined as  $c = (A^-/\alpha)t^{-\alpha}$ ,  $t = 1 - T/T_c$  and  $\lambda_i^2 = \lambda_{i0}^2 t^{-\nu}$ , where  $\alpha$  and  $\nu$  are the critical exponents. Although  $T_c$ ,  $A^-$  and  $\lambda_{i0}^2$  depend on the dopant concentration, isotope exchange etc., universality implies that this combination does not. Hence this relation puts a crucial constraint on the microscopic theory of superconductivity in cuprates. To illustrate this point it is instructive to consider the doping dependence of  $T_c$ ,  $\lambda_{ab}^2 \simeq \lambda_{a0}\lambda_{b0}$ ,  $\gamma_0 = \lambda_{c0}/\lambda_{ab0}$  and  $A^-$  close to the 2D-QSI transition (see Fig.1). Here  $T_c$ ,  $1/\lambda_{ab0}^2$  and  $\gamma_0$  are known to scale as  $T_c \propto 1/\lambda_{ab0}^2 \propto 1/\gamma_0 \propto p - p_u$  so that the critical amplitude of the specific heat singularity vanishes according to Eq.(8) as  $A^- \propto (p - p_u)^2 \propto T_c^2$ . This is consistent with the specific heat data for underdoped  $\text{La}_{2-x}\text{Sr}_x\text{CuO}_4$  and underdoped  $\text{Tl}_2\text{Ba}_2\text{CuO}_{6+\delta}$  [53]. Furthermore, the universal relation implies that the relative changes upon isotope substitution satisfy the relation [54]

$$\frac{\Delta T_c}{T_c} = -\frac{\Delta A^-}{3A^-} - \frac{1}{3} \sum_{i=a,b,c} \frac{\Delta \lambda_{i0}^2}{\lambda_{i0}^2}. \quad (9)$$

It explains why close to the transition temperature and optimum doping ( $p = p_m$ ) a substantial isotope effect on the penetration depths is compatible with a negligible effect on  $T_c$ .

Approaching the 2D-XY-QSI transition in the underdoped regime (see Fig.1) a crossover to the universal relation [50]

$$T_c = \frac{\Phi_0^2 \bar{R}_2}{16\pi^3 k_B} \frac{d_s}{\lambda_{ab}^2(0)}, \quad (10)$$

takes place and the cuprates correspond to a stack of independent sheets of thickness  $d_s$ .  $\bar{R}_2$  is a universal number. The flow to 2D-XY-QSI behavior is experimentally well confirmed in terms of Uemura's plot [23]. It is a characteristic 2D property and also applies to the onset of superfluidity in  $^4\text{He}$  films adsorbed on disordered substrates where it is well confirmed [55]. Although  $T_c$ ,  $d_s$  and  $\lambda_{ab}^2(0)$  depend on dopant concentration, isotope substitution, etc., universality implies that this relation does not. This puts yet another constraint on the microscopic theory of superconductivity in the cuprates. Furthermore it yields for the relative changes upon isotope exchange the relation

$$\frac{\Delta T_c}{T_c} = \frac{\Delta d_s}{d_s} - \frac{\Delta \lambda_{ab}^2(0)}{\lambda_{ab}^2(0)}, \quad (11)$$

applicable close to the underdoped limit ( $p = p_u$ ). Although the experimental data are rather sparse in the underdoped regime [54,56], suggestive evidence for an isotope effect on the effective thickness  $d_s$  of the superconducting sheet emerges, namely  $\Delta d_s/d_s = (^{18}d_s - ^{16}d_s)/^{16}d_s \approx 0.03$  [54]. Estimates for  $d_s$  can be derived from the crossing point phenomenon in the temperature dependence of the magnetization for various applied magnetic fields, applied parallel to the c-axis. In a 3D anisotropic superconductor, falling into the 3D-XY universality class, the magnetization data plotted in terms  $m_z/H_z^{1/2}$  versus  $T$  will cross at  $T_c$ , where  $z$  is along the c-axis. Consistency with this behavior was found in a variety of cuprates [50]. On the contrary, in a 2D superconductor, corresponding to a slab of thickness  $d_s$ , the crossing point occurs in the plot  $m_z$  versus  $T$  at the Kosterlitz-Thouless transition temperature  $T_{KT}$ , where  $m_z \propto -k_B T_{KT}/(\Phi_0 d_s)$ . Even though bulk cuprates are strictly 2D only close to the 2D-QSI transition at  $p = p_u$  (see Fig.1), in the highly anisotropic materials, such as Bi-2212 and Tl-1223, 2D crossing point feature have been observed and used to estimate  $d_s$ , yielding values close to the c-axis lattice constant [50]. Since the lattice parameters remain essentially unaffected [29,30] by isotope exchange, while  $d_s$  does, the substantial relative change  $\Delta d_s/d_s = (^{18}d_s - ^{16}d_s)/^{16}d_s \approx 0.03$  [54] uncovers again the relevance of electron-lattice coupling. Going further, by combining Eqs.(7) and (11), extrapolated to the underdoped regime, we obtain the approximate relation

$$\frac{\Delta d_s}{d_s} = -\frac{\Delta \left( \widetilde{v_F/v_2} \right)}{\left( \widetilde{v_F/v_2} \right)}, \quad (12)$$

which provides additional evidence for the coupling between superconducting properties and lattice degrees of freedom. The approximate nature of this relation stems from the fact that the d-wave quasiparticle scenario does not hold down to the 2D-QSI transition due to the neglect of quantum fluctuations, associated with the phase of the order parameter. Indeed, the linear-in-T temperature dependence of  $1/\lambda_{ab}^2$  simply follows from the existence of a 2D-QSI transition. The result is,  $(\lambda_{ab}(0)/\lambda_{ab}(T))^2 - 1 \propto T/T_c$ , holds for d- and s-wave pairing [9].

Additional evidence for electron-lattice coupling emerges from the combined oxygen isotope and finite size effects. Due to inhomogeneities of extrinsic or intrinsic origin, cuprates are homogeneous over a finite extent only. Thus a

finite size effect [57] is expected to occur, whereby the correlation volume cannot grow beyond the volume of the homogeneous domains. When 3D-XY critical fluctuations dominate there is the universal relationship [50]

$$\frac{1}{\lambda_i(T)\lambda_j(T)} = \frac{16\pi^3 k_B T}{\Phi_0^2 \sqrt{\xi_i^t(T)\xi_j^t(T)}}, \quad (13)$$

between the London penetration depths  $\lambda_i$  and transverse correlation lengths  $\xi_i^t$  in directions  $i$  and  $j$ . In the presence of inhomogeneities with length scales  $L_i$  the  $\xi_i^t = \xi_{i0}^t |t|^{-\nu}$ , where  $t = T/T_c - 1$ , cannot diverge but are bounded by

$$\xi_i^t \xi_j^t \leq L_k^2, \quad i \neq j \neq k. \quad (14)$$

A characteristic feature of the resulting finite size effect is the occurrence of an inflection point at  $T_{pk}$  in  $1/\lambda_i(T)\lambda_j(T)$  below  $T_c$ , the transition temperature of the homogeneous system. Here

$$\xi_i^t(T_{pk})\xi_j^t(T_{pk}) = L_k^2, \quad i \neq j \neq k, \quad (15)$$

and Eq.(13) reduces to

$$\frac{1}{\lambda_i(T)\lambda_j(T)} \Big|_{T=T_{pk}} = \frac{16\pi^3 k_B T_{pk}}{\Phi_0^2} \frac{1}{L_k}. \quad (16)$$

In the homogeneous case  $1/(\lambda_i(T)\lambda_j(T))$  decreases continuously with increasing temperature and vanishes at  $T_c$ , while in the presence of inhomogeneities it exhibits an inflection point at  $T_{pk} < T_c$ , so that

$$d\left(\frac{1}{\lambda_i(T)\lambda_j(T)}\right)/dT \Big|_{T=T_{pk}} = 0 \quad (17)$$

Since the experimental data for the temperature dependence of the penetration depths is available in the form  $\lambda_{ab}$  and  $\lambda_c$  only, we rewrite Eq.(16) as

$$L_c = \frac{16\pi^3 k_B T_{pc} \lambda_{ab}^2(T_{pc})}{\Phi_0^2}, \quad L_{ab} = \frac{16\pi^3 k_B T_{pb} (\lambda_{ab}(T)\lambda_c(T))_{T=T_{pab}}}{\Phi_0^2}. \quad (18)$$

Apart from the inflection point, an essential characteristic of a finite size effect is the finite size scaling function [58]. In the present case and for  $\lambda_{ab}$  it is defined in terms of

$$\left(\frac{\lambda_{0ab}}{\lambda_{ab}(T)}\right)^2 |t|^{-\nu} = g_c(y), \quad y = \text{sign}(t) |t| \left(\frac{L_c}{\xi_{0ab}^t}\right)^{1/\nu} = \text{sign}(t) \left|\frac{t}{t_{pc}}\right| \quad (19)$$

For  $t = T/T_c - 1$  small and  $L_c \rightarrow \infty$ , so that  $\pm y \rightarrow \infty$ , it should tend to  $g_c(y \rightarrow -\infty) = 1$  and  $g_c(y \rightarrow \infty) = 0$ , respectively, while for  $t = 0$  and  $L_c \neq 0$  it diverges as

$$g_c(y \rightarrow 0) = g_{0c} |y|^{-\nu} = g_{0c} \left|\frac{t}{t_{pc}}\right|^{-\nu}, \quad (20)$$

whereby  $(\lambda_{0ab}/\lambda_{ab}(T_c, L))^2 = g_{0c} |t_{pc}|^\nu = g_{0c} \xi_{0ab}^t / L_c$ . As expected, a sharp superconductor to normal state transition requires domains of infinite extent. Moreover at  $t_{pc}$ ,  $y = 1$  and there is an inflection point because  $d(\lambda_{0ab}/\lambda_{ab}(T, L))^2/dt = 0$ . Since the scaling function  $g_c(y)$  depends on the type of confining geometry and on the conditions imposed (or not, in the case of free boundaries) at the boundaries of the domains, this applies to the amplitude  $g_{0c}$  as well. In Fig.2a we displayed the microwave surface impedance data for  $\lambda_{ab}^2(T=0)/\lambda_{ab}^2(T)$  and  $d(\lambda_{ab}^2(T=0)/\lambda_{ab}^2(T))/dT$  versus  $T$  of a high-quality  $\text{Bi}_2\text{Sr}_2\text{CaCu}_2\text{O}_{8+\delta}$  single crystal taken from Jacobs *et al.* [59]. The solid curve indicates the leading 3D-XY critical behavior of the homogeneous system, while the data uncovers a rounded transition which occurs smoothly. This behavior, together with the occurrence of an inflection point around  $T_{pc} \approx 87\text{K}$ , where  $d(\lambda_{ab}^2(T=0)/\lambda_{ab}^2(T))/dT$  exhibits an extremum, points to a finite size effect. With  $\lambda_{ab}(T=0) = 1800\text{\AA}$  obtained from  $\mu\text{SR}$  measurements [60],  $T_{pc} \approx 87\text{K}$  and  $\lambda_{ab}^2(T=0)/\lambda_{ab}^2(T_{pc}) = 0.066$  we obtain with the aid of Eq.(18) the estimate  $L_c \approx 68\text{\AA}$ . Although the spatial extent of the homogeneous domains along the c-axis appears to be of nanoscale only, the small critical amplitude of the transverse correlation length,

$\xi_{0ab}^t = L_c (1 - T_{pc}/T_c)^{2/3} \approx 2.2\text{\AA}$ , makes the 3D-XY critical regime  $(\lambda_{ab}^2(0)/\lambda_{ab}^2(T) \propto (1 - T/T_c)^{2/3})$  attainable. An additional and essential characteristic of a finite size effect appearing in the temperature dependence of the in-plane penetration depth is the consistency of  $(\lambda_{0ab}/\lambda_{ab}(T))^2 |t|^{-\nu}$  versus  $t/|t_{pc}|$  with the shape and limiting behavior of the finite size scaling function (see Eq.(19)). In Fig.2b we displayed  $(\lambda_{0ab}/\lambda_{ab}(T))^2 |t|^{-\nu}$  versus  $t/|t_{pc}|$ . The apparent agreement with the aforementioned characteristic behavior of this function, provides strong evidence for a finite size effect, due to the limited extent  $L_c$  of homogeneous superconducting domains along the c-axis. Clearly, such a finite size scaling analysis, performed on one set of data for one particular sample and material only, cannot distinguish between an intrinsic or extrinsic origin of the inhomogeneity. Noting that this behavior was found in a variety of cuprates and for data obtained with different techniques [61], one is lead to the conclusion that inhomogeneities, giving rise to a finite size effect, are yet another facet of the mystery of superconductivity in the cuprates. Clearly this finite size effect is not restricted to the penetration depth but should be visible in other thermodynamic properties. In the specific heat it leads to a rounding of the peak and its consistency with a finite size effect was established for the data taken on  $\text{YBa}_2\text{Cu}_3\text{O}_{7-\delta}$  high quality single crystals [50]. In these samples the domain size was found to range from 300 to 400 Å. Furthermore nanoscale spatial variations in the electronic characteristics have also been observed in underdoped  $\text{Bi}_2\text{Sr}_2\text{CaCu}_2\text{O}_{8+\delta}$  with scanning tunnelling microscopy (STM) [62–65]. They reveal a spatial segregation of the electronic structure into 3nm diameter superconducting domains in an electronically distinct background.

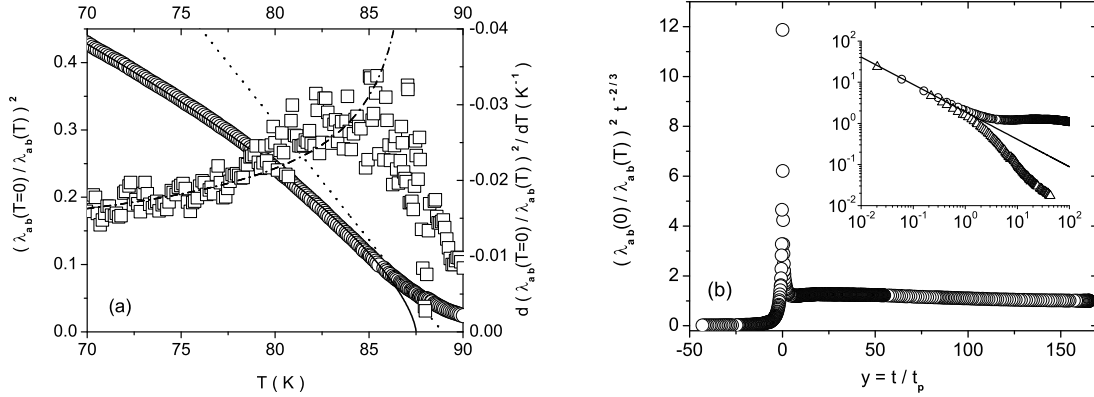


FIG. 2. (a) Microwave surface impedance data for  $\lambda_{ab}^2(T=0)/\lambda_{ab}^2(T)$  (○) and  $d(\lambda_{ab}^2(T=0)/\lambda_{ab}^2(T))/dT$  (□) versus  $T$  of a high-quality  $\text{Bi}_2\text{Sr}_2\text{CaCu}_2\text{O}_{8+\delta}$  single crystal taken from Jacobs *et al.* [59]. The solid line is  $\lambda_{ab}^2(0)/\lambda_{ab}^2(T) = 1.2(1 - T/T_c)^{2/3}$  and the dash-dot line its derivative with  $T_c = 87.5\text{K}$ , indicating the leading critical behavior of the homogeneous system. The dotted line is the tangent to the inflection point at  $T_p \approx 87\text{K}$ , where  $d(\lambda_{ab}^2(0)/\lambda_{ab}^2(T))/dT$  is maximum; (b) Finite size scaling function  $g(y) = (\lambda_{0ab}/\lambda_{ab}(T))^2 |t|^{-\nu}$  versus  $y = t/|t_p|$  for the data shown in Fig.2a. The solid line in the inset is Eq.(19) with  $g_{0c} = 1.6$ .

Supposing that the limiting length scales change upon isotope exchange, we obtain from Eq.(18) the relation

$$\frac{\Delta T_{pc}}{T_{pc}} = \frac{\Delta L_c}{L_c} - \frac{\Delta \lambda_{ab}^2(T_{pc})}{\lambda_{ab}^2(T_{pc})}, \quad (21)$$

which matches Eq.(11), applicable in the 2D limit where the limiting length is set by  $d_s$ , the thickness of the independent sheets. Furthermore, this relation opens the possibility to probe the coupling between superfluidity and lattice degrees of freedom close to criticality, where mean-field treatments fail. Indeed, given the fact that the lattice parameters remain essentially unaffected [29,30] by isotope exchange, a purely electronic mechanism requires  $\Delta L_c = 0$ . The effect of oxygen isotope substitution on the inhomogeneity induced finite size effect has been explored in  $\text{Y}_{1-x}\text{Pr}_x\text{Ba}_2\text{Cu}_3\text{O}_{7-\delta}$  [66]. From the resulting estimates, listed in Table II, several observations emerge. First,  $L_c$  increases systematically with reduced  $T_{pc}$ . Second,  $L_c$  grows with increasing  $x$  and upon isotope exchange ( $^{16}\text{O}$ ,  $^{18}\text{O}$ ). Third, the relative shift of  $T_{pc}$  is very small. This reflects the fact that the change of  $L_c$  is essentially due to the superfluid, probed in terms of  $1/\lambda_{ab}^2$ . Accordingly,  $\Delta L_c/L_c \approx \Delta \lambda_{ab}^2(T_{pc})/\lambda_{ab}^2(T_{pc})$  for  $x = 0, 0.2$  and  $0.3$ .

x	0	0.2	0.3
$\Delta T_{p_c}/T_{p_c}$	-0.000(2)	-0.015(3)	-0.021(5)
$\Delta L_c/L_c$	0.12(5)	0.13(6)	0.16(5)
$\Delta \lambda_{ab}^2(T_{p_c})/\lambda_{ab}^2(T_{p_c})$	0.11(5)	0.15(6)	0.15(5)
$^{16}T_{p_c}(K)$	89.0(1)	67.0(1)	52.1(2)
$^{18}T_{p_c}(K)$	89.0(1)	66.0(2)	51.0(2)
$^{16}L_c(\text{\AA})$	9.7(4)	14.2(7)	19.5(8)
$^{18}L_c(\text{\AA})$	10.9(4)	16.0(7)	22.6(9)

Table II: Finite size estimates for  $\Delta T_{p_c}/T_{p_c}$ ,  $\Delta L_c/L_c$ ,  $\Delta \lambda_{ab}^2(T_{p_c})/\lambda_{ab}^2(T_{p_c})$ ,  $^{16}T_{p_c}$ ,  $^{18}T_{p_c}$ ,  $^{16}L_c$  and  $^{18}L_c$  for an  $^{18}\text{O}$  content of 89% taken from [66].

To appreciate the implications of these estimates, we note again that for fixed Pr concentration the lattice parameters remain essentially unaffected [29,30]. Accordingly, an electronic mechanism, without coupling to lattice degrees of freedom implies  $\Delta L_c = 0$ . On the contrary, a significant change of  $L_c$  upon oxygen exchange uncovers the coupling between the superfluid, probed by  $\lambda_{ab}^2$ , and the oxygen lattice degrees of freedom. A glance to Table II shows that the relative change of the superconducting domains along the c-axis upon oxygen isotope exchange is significant, ranging from 12 to 16%, while the relative change of the inflection point  $T_{p_c}$  is an order of magnitude smaller. For this reason the significant relative change of  $L_c$  at fixed Pr concentration is accompanied by essentially the same relative change of  $\lambda_{ab}^2$ , which probes the superfluid. This uncovers unambiguously the existence and relevance of the coupling between the superfluid and oxygen lattice degrees of freedom. Furthermore, this behavior agrees with the isotope effect on  $d_s$  [54], the limiting length scale close to the 2D-QSI transition. Potential candidates for the relevant lattice degrees of freedom are the Cu-O bond-stretching-type phonons showing temperature dependence, which parallels that of the superconductive order parameter [67].

An additional probe to unravel the mystery of superconductivity in the cuprates is the response to a magnetic field. In the early discussion of the symmetry of the order parameter, Yip and Sauls [68] proposed that the angular position of the gap nodes could be probed by a measurement of the magnetic field dependence of the penetration depth. In the local limit and for  $T \rightarrow 0$ , they predicted the linear relationship,  $(\lambda(H=0, T=0)/\lambda(H, 0))^2 - 1 \propto -H$ , where the factor of proportionality is independent of temperature. Several experimental groups tried to verify this prediction, but failed to identify a linear  $H$  term which scaled with temperature according to the theory [69–72]. On the other hand, calculations based on a d-wave model, treated in the quasi classical approximation, suggest that  $(\lambda(H=0, T=0)/\lambda(H, 0))^2 - 1 \propto -\sqrt{H}$  [74]. However, in these treatments fluctuations have been neglected. Close to the phase transition line  $T_c(p)$ , where thermal fluctuations dominate, the in-plane penetration depth scales as  $\lambda_{ab}^2 \propto \xi_c = \xi_{ab}/\gamma$ , while the magnetic field applied parallel to the c-axis scales as  $H_c \propto \Phi_0/\xi_{ab}^2$ . Thus the in-plane penetration satisfies at  $T_c$  the scaling form

$$\frac{1}{\lambda_{ab}^2(T_c, H_c)} \propto \sqrt{H_c}, \quad (22)$$

revealing that a superconductor is dramatically influenced by an applied magnetic field. This behavior can be understood by noting that in an applied magnetic field the correlation length cannot grow indefinitely. For nonzero magnetic field  $H_c$  there is the limiting length scale  $L_{H_c} \simeq \sqrt{\Phi_0/(aH_c)}$  with  $a \simeq 3.12$  [61], related to the average distance between vortex lines. Indeed, as the magnetic field increases the density of vortex lines becomes greater, but this cannot continue indefinitely. The limit is roughly set on the proximity of vortex lines by the overlapping of their cores. Due to this limiting length scale the phase transition of a homogeneous superconductor is rounded and occurs smoothly. At  $T = 0$  and close to the 2D-QSI transition the in-plane penetration depth scales as  $\lambda_{ab}^2 \propto \xi_{ab}^z$ , where  $z$  is the dynamic critical exponent of this transition. With  $H_c \propto \Phi_0/\xi_{ab}^2$  this yields the scaling form

$$\left( \frac{\lambda(0, 0)}{\lambda(H_c, T=0)} \right)^2 - 1 \propto -H_c^{z/2}. \quad (23)$$

Contrariwise at  $T = 0$  and close to the 3D-QSN transition the in-plane penetration depth scales as  $\lambda_{ab}^2 \propto \xi_{ab}^{z+1}$  so that

$$\left( \frac{\lambda(0, 0)}{\lambda(H_c, T=0)} \right)^2 - 1 \propto -H_c^{(z+1)/2}. \quad (24)$$



Since the order parameter is assumed to be a complex scalar, these scaling forms hold for both, s-wave and d-wave pairing. Taking the evidence for a 2D-QSI transition with  $z = 1$  and a 3D-QSN transition with  $z = 2$  into account [4], the scaling form  $(\lambda(H=0, T=0)/\lambda(H,0))^2 - 1 \propto -\sqrt{H_c}$  is expected to hold in the underdoped regime, while in the overdoped limit  $(\lambda(H=0, T=0)/\lambda(H,0))^2 - 1 \propto -H_c^{3/2}$  should apply. In any case more extended experimental investigations are required, including samples covering the full doping range, to overcome the present impasse. Another property suite to shed light on the critical properties of the quantum transitions is the magnetic field dependence of the zero temperature specific heat coefficient. At  $T = 0$  and close to the 2D-QSI or 3D-QSN transitions it scales as  $(c/T)_{T=0} \propto \xi_{ab}^{D-z} \propto H_c^{(D-z)/2}$ . The data taken on  $\text{La}_{2-x}\text{Sr}_x\text{CuO}_4$  [75] points to  $(D-z)/2 \simeq 1/2$ , irrespective of the dopant concentration. This suggests respectively,  $z = 1$  for the 2D-QSI and  $z = 2$  for the 3D-QSN transition.

The doping dependence of the zero temperature penetration depths provides another link between the quantum critical behavior in the underdoped and overdoped regimes. In Fig.3 we displayed  $1/\lambda_{ab}^2(0)$  versus  $p \simeq x$  for  $\text{La}_{2-x}\text{Sr}_x\text{CuO}_4$  taken from Panagopoulos *et al.* [76]. Close to the quantum phase transitions  $1/\lambda_{ab}^2(0)$  scales as  $1/\lambda_{ab}^2(0) \propto \delta^{\bar{\nu}(D+z-2)}$  [50], where  $\delta = p - p_u$  at the 2D-QSI and  $\delta = p_o - p$  at the 3D-QSN transition. The solid line indicates the crossover from a 2D-QSI transition with  $z = \bar{\nu} = 1$  to a 3D-QSN transition with  $z = 2$  and  $\bar{\nu} = 1/2$ . While the flow to the 2D-QSI transition is apparent, the data does not extend sufficiently close to 3D-QSN criticality to confirm this crossover unambiguously. In any case, it emerges that the properties of the ground state are controlled by the crossover from the 2D-QSI to the 3D-QSN critical point. For this reason it can be understood that away from these quantum critical points, around optimum doping ( $p = p_m$ , see Fig.1), quantum fluctuations are suppressed to the extent that Bogoliubov quasi-particle features are observable and mean-field treatments represent a reasonable starting point. A 2D-QSI transition with  $z = 1$  and  $\bar{\nu} = 1$  coincides with the theoretical prediction for a 2D disordered bosonic system with long-range Coulomb interactions [77–79]. A potential candidate for 3D-QSN criticality is the disordered d-wave superconductor to disordered metal transition at weak coupling considered by Herbut [80] [38], with  $z = 2$  and  $\bar{\nu} = 1/2$ . energy. Here the disorder destroys superconductivity, while at the 2D-QSI transition it localizes the pairs.

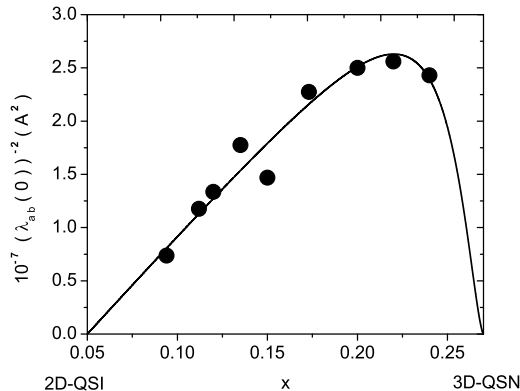


FIG. 3.  $1/\lambda_{ab}^2(0)$  versus  $p \simeq x$  for  $\text{La}_{2-x}\text{Sr}_x\text{CuO}_4$ . •: experimental data taken from Panagopoulos *et al.* [76] The solid line indicate the crossover from a 2D-QSI transition with  $z = \bar{\nu} = 1$  to a 3D-QSN transition with  $z = 2$  and  $\bar{\nu} = 1/2$ .

To summarize, in the regime where mean-field treatments are expected to apply, the substantial isotope effect on the zero temperature penetration depth, established by a variety of experimental techniques, implies a renormalization of the normal state Fermi velocity due to a electron-lattice coupling, beyond the band velocity and the ME theory. This coupling also affects the superconducting properties and should be observable with ARPES. Close to the critical line  $T_c(p)$  and the critical endpoints, either thermal or quantum fluctuations, not included in mean-field treatments, dominate. In these regions of the phase diagram the theory of quantum and thermal critical phenomena applies. Given the universality class of the respective transition, there are universal relations between critical properties, putting stringent constraints on the microscopic theory of superconductivity in the cuprates. Along the phase transition line there is in the experimentally accessible temperature regime mounting evidence for 3D-XY universality and for a 3D-2D- crossover as the underdoped limit is approached. Here a 2D-QSI transition occurs. This crossover, measured in terms of the ratio  $\gamma = \lambda_c/\lambda_{ab}$  (see Fig.1) is well documented [3,4] and implies that superconductivity in the cuprates is a genuine 3D phenomenon. The resulting competition between anisotropy and superconductivity raises serious doubts whether 2D mechanisms and models, corresponding to the limit  $\gamma = \infty$ , can explain the essential

observations of superconductivity in the cuprates. Indeed, as the dopant concentration is increased, the cuprates undergo in the ground state a crossover from 2D-QSI to 3D-QSN criticality. For this reason the observation of Bogoliubov quasi-particle features far away from these quantum critical points, around optimum doping ( $p = p_m$ , see Fig.1), can be understood. Here quantum fluctuations do not dominate. Yet another facet of the mystery emerges from the evidence for a finite size effect in the temperature dependence of the in-plane penetration depth. Although the limiting length scales may depend on the history of the sample, their dependence on oxygen isotope substitution reveals and confirms the coupling between superconducting properties and lattice degrees of freedom. Although the majority opinion on the mechanism of superconductivity in the cuprates is that it occurs via a purely electronic mechanism, and lattice degrees of freedom are supposed to be irrelevant, we have shown that the oxygen isotope effect on the in-plane penetration depth uncovers yet another facet, the hitherto ignored coupling between lattice degrees of freedom and both, normal state and superconducting state properties, the existence of inhomogeneities giving rise to a finite size effect. Finally we note that a variety of other properties also display pronounced phonon and electron-lattice effects: superconductivity-induced lattice changes [45,51,73,81,82], superconductivity-induced phonon renormalization [67,83–87], tunnelling phonon structures [88,89], etc., give additional evidence of significant electron-lattice coupling. Furthermore we have seen that the occurrence of power law terms in the low temperature and low magnetic field dependence of the in-plane penetration depth do not necessarily single out d-wave pairing, but stem from fluctuations at work, associated with a complex scalar order parameter which is compatible with both, s- and d-wave pairing.

### ACKNOWLEDGMENTS

The author is grateful to M. Cohen, R. Khasanov, H. Keller, K.A. Müller and D. R. Nelson for very useful comments and suggestions on the subject matter, and to Claudia Ambrosch-Draxl and R. Zeyher for clarifying correspondence.

- 
- [1] J. L. Tallon *et al.*, Phys. Rev. B **51**, 12911 (1995).
  - [2] M.R. Presland *et al.*, Physica C **176**, 95 (1991).
  - [3] T. Schneider, Europhys. Lett. **60**, 141 (2002).
  - [4] T. Schneider, Physica B **326**, 289 (2003).
  - [5] B. S. Chandrasekhar and D. Einzel, Annalen der Physik **2**, 535 (1993).
  - [6] P. J. Hirschfeld and N. Goldenfeld, Phys. Rev. B **48**, 4219 (1993).
  - [7] A. C. Durst and P. A. Lee, Phys. Rev. B **62**, 1270, (2000).
  - [8] W. N. Hardy, D. A. Bonn, D. C. Morgan, R. Liang, and K. Zhang, Phys. Rev. Lett. **70**, 3999 (1993).
  - [9] T. Schneider<sup>1</sup> and J. M. Singer, J. of Superconductivity, **13**, 789 (2000).
  - [10] J. A. Martindale, S. E. Barrett, K. E. OHara, C. P. Slichter, W. C.Lee, and D. M. Ginsberg, Phys. Rev. B **47**, 9155 (1993).
  - [11] P. A. Lee, Phys. Rev. Lett. **71**, 1887 (1993).
  - [12] M. J. Graf, S-K. Yip, J. A. Sauls, and D. Rainer, Phys. Rev. B **53**, 15147 (1996).
  - [13] L. Taillefer, B. Lussier, R. Gagnon, K. Behnia, and H. Aubin, Phys. Rev. Lett. **79**, 483 (1997).
  - [14] K. A. Moler, D. L. Sisson, J. S. Urbach, M. R. Beasley, A. Kapitulnik, D. J. Baar, R. Liang, and W. N. Hardy, Phys. Rev. B **55**, 3954 (1997).
  - [15] D. A. Wright, J. P. Emerson, B. F. Woodfield, J. E. Gordon, R. A. Fisher, and N. E. Phillips, Phys. Rev. Lett. **82**, 1550 (1999).
  - [16] Y. Wang *et al.*, Phys. Rev. B **63**, 094508 (2001).
  - [17] M. Tinkham, *Introduction to Superconductivity*, McGraw Hill, New York 1975.
  - [18] G. Zhao, V. Kirtikar, and D.E. Morris, Phys. Rev. B **63**, 024503(2001).
  - [19] J. Hofer *et al.*, Phys. Rev. Lett. **84**, 4192 (2000).
  - [20] R. Khasanov *et al.*, J. Phys. Condensed Matter **15**, L17 (2003).
  - [21] R. Khasanov *et al.*, cond-mat/0305477.
  - [22] J. L. Tallon *et al.*, cond-mat/0211071.
  - [23] Y. J. Uemura, Solid State Communications **126**, 2338 (2003)
  - [24] D. DiCastro *et al.*, cond-mat/0307330.
  - [25] W. E. Pickett, Rev. Mod. Phys. **61**, 433 (1989).
  - [26] J.C. Campuzano, M.R. Norman, and M. Randeria, cond-mat/0209476.

- [27] A. Lanzara *et al.*, Nature **420**, 511 (2001).
- [28] S. F. Lee *et al.*, Phys. Rev. B **53**, 11825 (1996).
- [29] K. Conder *et al.*, in *Phase Separation in Cuprate Superconductors*, edited by E. Sigmund and K. A. Muller (Springer, Berlin 1994) p. 210.
- [30] F. Raffa *et al.*, Phys. Rev. Lett. **81**, 5912 (1998).
- [31] N. L. Wang *et al.*, Phys. Rev. Lett. **89**, 087003 (2002).
- [32] T. Biggs *et al.*, cond -mat/0203392.
- [33] A. B. Migdal, Sov. Phys. JETP **7**, 996 (1958); G. M. Eliashberg, Sov. Phys. JETP **11**, 696 (1960).
- [34] E.I. Maksimov, Zh. Eksp.Teor. Fiz. **37**, 1562 (1969).
- [35] J. P. Carbotte, Rev. Mod. Phys. **62**, 1027 (1990).
- [36] A. Paramekanti, M. Randeria, and N. Trivedi, cond-mat/0305611.
- [37] A. Deppeler and A. J. Millis, Phys. Rev. B **65**, 100301 (2002).
- [38] A. Deppeler and A. J. Millis, Phys. Rev. B **65**, 224301 (2002).
- [39] D.S. Fisher, M.P.A. Fisher, and D.A. Huse, Phys. Rev. B **43**, 130 (1991).
- [40] T. Schneider and H. Keller, Int. J. Mod. Phys. B **8**, 487 (1993).
- [41] N. Overend, M.A. Howson, and I.D. Lawrie, Phys. Rev. Lett. **72**, 3238 (1994).
- [42] M. A. Hubbard *et al.*, Physica C **259**, 309 (1996).
- [43] S. Kamal *et al.*, Phys. Rev. Lett. **73**, 1845 (1994).
- [44] S. Kamal *et al.*, , Phys. Rev. B **58**, 8933 (1998).
- [45] V. Pasler *et al.*, Phys. Rev. Lett. **81**, 1094 (1998).
- [46] T. Schneider, J. Hofer, M. Willemin, J.M. Singer, and H. Keller, Eur. Phys. J. B **3**, 413 (1998).
- [47] T. Schneider and J. M. Singer, Physica C **313**, 188 (1999).
- [48] J. Hofer *et al.*, Phys. Rev. B **60**, 1332 (1999, B **62**, 631 (2000)
- [49] T. Schneider and J. S. Singer, Physica C **341-348**, 87 (2000)
- [50] T. Schneider and J. M. Singer, *Phase Transition Approach To High Temperature Superconductivity*, Imperial College Press, London, 2000.
- [51] C. Meingast *et al.*, Phys. Rev. Lett. **86**, 1606 (2001).
- [52] K. D. Osborn, D. J. Van Harlingen, Vivek Aji, N. Goldenfeld, S. Oh, and J. N. Eckstein, cond-mat/0204417
- [53] J. W. Loram *et al.*, Physica C **235-240**, 134 (1994).
- [54] T. Schneider, Phys. Rev. B **67**, 134514 (2003).
- [55] P.A. Crowell, F.W. van Keuls, J.R. Reppy, Phys. Rev. B **55**, 12620 (1997).
- [56] T. Schneider and H. Keller, Phys. Rev. Lett. **82**, 4899 (2001).
- [57] M. E. Fisher and M. N. Barber, Phys. Rev. Lett. **28** 1516 (1972); M. E. Fisher, Rev. Mod.Phys. **46**, 597 (1974); V. Privman, *Finite Size Scaling and Numerical Simulation of Statistical Systems*, World Scientific, Singapore 1990.
- [58] N. Schultka and E. Manousakis, Phys. Rev. Lett. **75**, 2710 (1995).
- [59] T. Jacobs, S. Sridhar, Q. Li, G. D. Gu, N. Koshizuka, Phys. Rev. Lett. **75**, 4516 (1995)
- [60] S. F. Lee *et al.*, Phys. Rev. Lett. **71**, 3862 (1993)
- [61] T. Schneider, cond-mat/0306668.
- [62] J. Liu, J. Wan, A. Goldman, Y. Chang and P. Jiang, Phys. Rev.Lett. **67**, 2195 (1991).
- [63] A. Chang, Z. Rong, Y. Ivanchenko, F. Lu and E. Wolf, Phys. Rev. B **46**, 5692 (1992).
- [64] T. Cren, D. Roditchev, W. Sacks, J. Klein, J.-B. Moussy, C. Deville-Cavellin, and M. Laguës, Phys. Rev. Lett. **84**, 147 (2000).
- [65] K. M. Lang, V. Madhavan, J. E. Hoffman, E. W. Hudson, H. Eisaki , S. Uchida and J. C. Davis, Nature **415**, 413 (2002).
- [66] T. Schneider, R. Khasanov, K. Conder and H. Keller, cond-mat/0302403.
- [67] J.-H. Chung *et al.*, Phys. Rev. B **67**, 014517 (2003).
- [68] S. K. Yip and J. A. Sauls, Phys. Rev. Lett. **69**, 2264 (1992).
- [69] A. Maeda, Y. Iino, T. Hanaguri, N. Motohira, K. Kishio, and T.Fukase, Phys. Rev. Lett. **74**, 1202 (1995); A. Maeda, T. Hanaguri, Y. Iino, S. Masuoka, Y. Kakata, J. Shimoyama, K. Kishio, H. Asaoka, Y. Matsushita, M. Hasegawa, and H. Takei, J. Phys. Soc. Jpn. **65**, 3638 (1996).
- [70] A. Carrington, R. W. Giannetta, J. T. Kim, and J. Giapintzakis, Phys. Rev. B **59**, 14 173 (1999).
- [71] C. P. Bidinosti, W. N. Hardy, D. A. Bonn, and Ruixing Liang, Phys. Rev. Lett. **83**, 3277 (1999).
- [72] J. E. Sonier, J. H. Brewer, R. F. Kiefl, G. D. Morris, R. I. Miller, D. A. Bonn, J. Chakhalian, R. H. Heffner, W. N. Hardy, and R. Liang, Phys. Rev. Lett. **83**, 4156 (1999).
- [73] H. You, U. Welp and Y. Fang, Phys. Rev. B **43**, 3660 (1991).
- [74] S. G. Sharapov, V. P. Gusynin and H. Beck, Phys. Rev. B **66**, 012515 (2002).
- [75] S. J. Chen, *et al.*, Phys. Rev. B **58**, 14573 (1998).
- [76] C. Panagopoulos, T. Xiang, W. Anukool, J. R. Cooper, Y. S. Wang, and C. W. Chu, Phys. Rev. B **67**, 220502 (2003).
- [77] M. P. A. Fisher, *et al.*, Phys. Rev. Lett. **64**, 587 (1990).
- [78] M. C. Cha, M. P. A. Fisher, S. M. Girvin, M. Wallin, P. A. Young, Phys. Rev. B **44**,6883 (1991).
- [79] I. F. Herbut, Phys. Rev. B **61**, 14723 (2000).
- [80] F.Herbut, Phys.Rev.Lett.**85**, 1532 (2000).

- [81] O. Chmaissem, J. D. Jorgensen, S. Short, A. Knizhnik, Y. Eckstein and H. Shaked, *Nature* **397**, 45 (1999).
- [82] N. L. Sani, A. Bianconi and A. Oyanagi, *J. Phys. Soc. Jap.* **70**, 2092 (2001).
- [83] L. Pintschovius and W. Reichardt, in *Physical Properties of High Temperature Superconductors IV*, edited by D. Ginsberg, (World Scientific, Singapore, 1994), p. 295.
- [84] T. Egami and S. J. L. Billinge, in *Physical Properties of High Temperature Superconductors V*, edited by D. Ginsberg, (World Scientific, Singapore, 1996), p. 265.
- [85] V.G. Hadjiev, X.J. Zhou, T. Strohm, M. Cardona, Q.M. Lin, and C.W. Chu, *Phys. Rev. B* **58**, 1043 (1998).
- [86] H. A. Mook and F. Dogan, *Nature (London)* **401**, 145 (1999).
- [87] A. Lanzara, P. V. Bogdanov, X. J. Zhou, S. A. Keller, D. L. Feng, E. D. Lu, T. Yoshida, H. Eisaki, A. Fujimori, K. Kishio, J.-Shimoyama, T. Noda, S. Uchida, Z. Hussain, and Z.-X. Shen, *Nature (London)* **412**, 510 (2001).
- [88] D. Shimada, Y. Shiina, A. Mottate, Y. Ohyagi, and N. Tsuda, *Phys. Rev. B* **51**, R16495 (1995).
- [89] R.S. Gonnelli, G.A. Ummarino and V.A. Stepanov, *Physica C* **275**, 162 (1997).